Tunable nonlinear damping in MoS$_2$ nanoresonator ⊘

Parmeshwar Prasad ✉ iD ; Nishta Arora; A. K. Naik ✉ iD

Check for updates

View Online

Export Citation

CrossMark
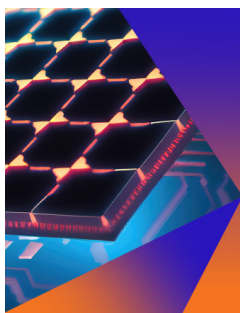
Applied Physics Letters

Special Topic:
Hybrid and Heterogeneous Integration in Photonics:
From Physics to Device Applications

Submit Today

AIP Publishing

AIP Publishing

Tunable nonlinear damping in MoS$_2$ nanoresonator

View Online   Export Citation   CrossMark

Parmeshwar Prasad,[a] (iD) Nishta Arora, and A. K. Naik[a] (iD)

AFFILIATIONS

Centre for Nano Science and Engineering, Indian Institute of Science, Bangalore 560012, India

[a]Authors to whom correspondence should be addressed: parmeshwar89@gmail.com and anaik@iisc.ac.in

ABSTRACT

Nonlinear damping plays a significant role in several areas of physics, including the dynamics of nanoresonators. However, many aspects remain unclear, and the microscopic source of nonlinear damping is still an active area of research. In particular, the effect of mode coupling on the observed damping has drawn significant interest. Here, we report on the effect of mode coupling on nonlinear damping in a highly tunable MoS$_2$ nano-mechanical drum resonator. In our experiments, we observe enhanced nonlinear damping in the parameter space that favors internal resonance. We observe this enhanced damping both in the direct drive and the parametric drive measurements. The study presents a comprehensive characterization of the tunable nonlinear damping of a MoS$_2$ resonator in a parametric regime. Our work marks a significant advancement in understanding the potential sources of nonlinear damping. Moreover, a highly tunable 2D material based nanoresonator offers an excellent platform to study nonlinear physics and exploit tunable nonlinear damping.

Published under an exclusive license by AIP Publishing. https://doi.org/10.1063/5.0177422

The dynamical motion of a system is intricately related to energy exchange with other entities. There are several ways through which a system accomplishes this energy exchange with its surroundings. In many cases, this exchange is dissipative and is modeled as linear damping in the simplest of cases. Some common damping mechanisms are thermoelastic damping, surface loss, loss through defects, clamping loss, and loss through coupling.[1–5] However, many other systems exhibit dissipative phenomena, which are nonlinear.[6–8] Nanomechanical systems are one such system wherein nonlinear dissipation has been observed.[7–10] In general, the effects of nonlinear dissipation are minute and are observed when vibration amplitudes are large[11] or if the other dominant effects are minimized.[12]

A clear understanding of the origin of nonlinear damping and its impact on dynamics is critical and is of interest due to its importance in biology,[13] magnetization,[14] quantum optics,[15] quantum oscillators,[16] and quantum information technologies.[17] Advancement in the fabrication and transduction technologies in the nanomechanical system in the last decade has led to exploration of these nonlinear dissipation mechanisms.[5,7–9,18–20] The nonlinear dissipation term can be included in the equation of motion in terms of the type $\eta z \dot{z}$, $\eta z^2 \dot{z}$, or $\eta \dot{z}^3$, where η is the nonlinear damping coefficient, z is the displacement, and $\dot{z}$ is the velocity.[11,21,22] The most accepted and tested term is $\eta z^2 \dot{z}$ in micro/nanoresonators and we aim to probe this nonlinear damping term in our nano-resonator. Though there are several models explaining the microscopic origin of nonlinear damping, the precise mechanism is not very well understood.[18,23,24] This is partly due to the

challenges in isolating and decoupling the nonlinear damping mechanism from other nonlinear effects. 2D materials based nanoresonators with an ultra-thin profile and tunable properties are fantastic tools for exploring nonlinear effects, including the nonlinear damping effects and their origin. In this context, a recent work by Keşkekler *et al.*[9] indicates the possible mechanism of the nonlinear damping through internal resonance (IR) in a graphene nanoresonator using optical actuation and detection technique. Damping through IR is a manifestation of loss through coupling mechanism within a resonator distinguishing itself from the more conventional viscous damping mechanisms.[1–4]

In this work, we observe the nonlinear IR damping mechanism in a molybdenum disulfide (MoS$_2$) device using the electrostatic homodyne capacitive actuation and detection method. The method provides a clean, fast, and simple platform to study the nonlinear system.[25,26] We employ two measurement techniques to investigate tunable nonlinear damping in our experiment, utilizing observation and characterization based on amplitude gain. Our results demonstrate enhanced control over nonlinear parameters compared to a prior similar experiment,[9] enabling decoupling of Duffing nonlinearity and probing nonlinear damping effectively. Our device shows two prominent modes with resonance frequency ω_1 and $\omega_2 \sim 2\omega_1$. The resonance frequencies of the two modes are highly tunable. This tunability provides a favorable tool to study the nonlinear damping in the parametric regime and probe the associated dissipation mechanisms. In our experiments, we tune the ratio of the resonance frequencies of the

two modes by changing the applied DC gate voltage. We observe that the effect of nonlinear damping increases considerably when the two modes are commensurate with each other in a 2:1 ratio. We examine the nonlinear damping in two distinct ways, first using direct drive where actuation force is applied close to the resonance frequency ($\omega \sim \omega_1$) and second using parametric pumping where force is applied close to twice the resonance frequency ($\omega \sim 2\omega_1$). Using the direct drive method, we monitor the dynamical response of mode 1 at constant actuation force while tuning the tension in the membrane with V_g^{dc}. We observe a change in the dissipation as the tension in the membrane changes. A clear enhancement in damping is observed when the conditions favor IR. To further probe this effect, we use the second method of parametric pumping. We observe that the effect of nonlinear damping manifests itself in parametric gain in the vicinity of IR. The parametric gain decreases by about six times when the nonlinear damping is maximum. We quantify the nonlinear damping and demonstrate that the enhancement is due to strong coupling between the two modes near internal resonance. The experiment sheds light on the mechanism of the nonlinear damping in highly tunable nanoresonators.

Our device is $\sim$6 layer thick MoS_2 drum resonator suspended over a $2\,\mu m$ diameter trench. The device is strained and actuated by applying voltage (V_g) to the gate electrode. The gate electrode is 300 nm below the suspended membrane. Figure 1(a) shows the schematic of the setup used to provide direct actuation, parametric pump and measure the displacement of the membrane. The membrane is strained by applying a DC gate voltage (V_g^{dc}) and actuated with an AC voltage (V_g^{ac}). The DC and the AC voltages are combined using a bias-tee before applying them to the gate electrode. Applied potential difference exerts a force on the suspended membrane, thereby displacing it from the equilibrium position. The displacement of the membrane modulates the geometric capacitance between the gate and the

membrane, leading to the change in voltage at the drain.[27,28] The change in drain voltage is amplified using a low-noise amplifier before measuring at the lock-in amplifier. Figures 1(b) and 1(c) show the frequency dispersion of two modes with applied DC gate voltage. We observe two distinct modes with similar frequency tuning with gate voltage. The frequencies of the two modes are $\omega_1 \sim 56\,MHz$ and $\omega_2 \sim 111\,MHz$ at around $V_g^{dc} = 23\,V$. The modes are interesting due to a 1:2 (i.e., $\omega_2 \sim 2\omega_1$) ratio of the frequencies, which enables us to achieve internal resonance. We can achieve a strong IR condition by tuning the DC gate voltage.

To obtain the elementary characteristics of the device, we drive it with fixed force ($F \propto V_g^{dc} V_g^{ac}$) over a range of gate voltages (V_g^{dc}). Varying the DC gate voltages enables us to modify the resonance frequencies of the modes while a constant force allows us to observe and compare the variation of amplitude response curve at different resonance frequencies. We drive the resonator with a force small enough to keep the response linear. The linear response can be quantified by the symmetry of the peak about the resonance frequency. In the nonlinear regime, a hysteresis in the frequency response curve is observed. Figure 2(a) shows amplitude response with frequency at different gate voltages. We observe that amplitude decreases with increase in DC gate voltage and reaches a minimum value around $V_g^{dc} \sim 22\,V$. In a linear system, a constant force should ideally result in a constant amplitude and linewidth due to linear dissipation. The observed reduction in amplitude for a constant applied force indicates enhanced dissipation. The linewidth of the response curve is shown in the Fig. 2(b). It shows that the damping is maximum at 22 V. Furthermore, as the driving force is increased, we observe the peak splitting around $V_g^{dc} = 23\,V$ to $V_g^{dc} = 24\,V$ [see Figs. 2(c) and 2(d)]. The splitting indicates coupling of this mode to one of the other vibrational modes.[29] The mode coupling can be enhanced by increasing the actuation force.
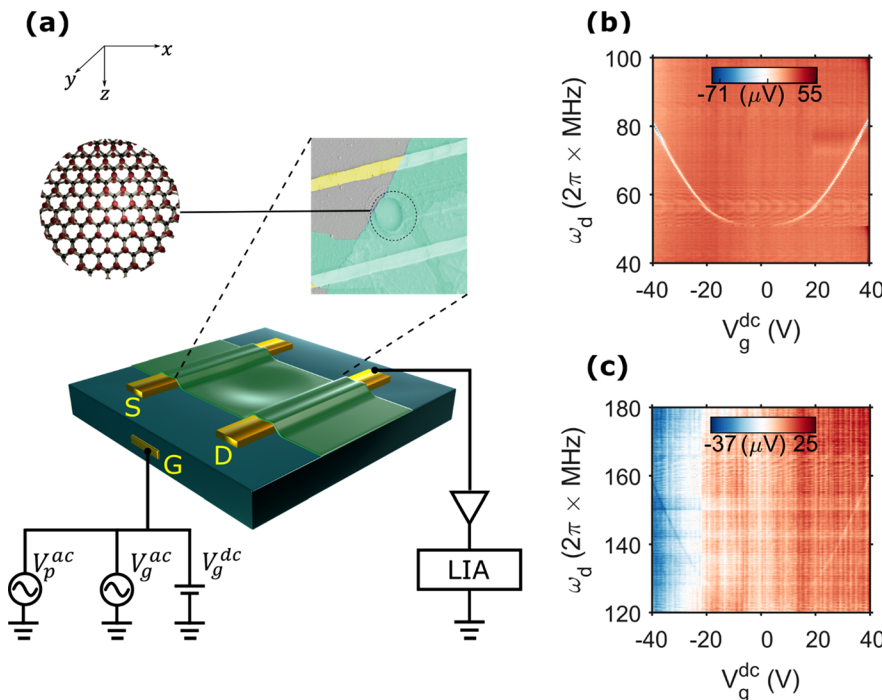
FIG. 1. Characterization of the device: (a) inset: SEM image of the device, the two thick yellow lines are source and drain electrodes, the suspended region is $2\,\mu m$ in diameter. The gate is 300 nm below the suspended membrane. Schematic of the measurement setup: homodyne capacitive actuation and detection technique. Membrane frequency is tuned using DC gate voltage V_g^{dc}, actuated directly using V_g^{ac} at frequency ω and parametrically at 2ω using V_p^{ac}. AC voltages are combined using RF power combiner, further DC is combined using a bias-tee. Readout is amplified using a low noise amplifier and measured at lock-in amplifier locked at ω. Frequency dispersion with V_g^{dc}, two modes ω_1 (b) and ω_2 (c) with frequency tuning >1 MHz/V and $\omega_2 \sim 2\omega_1$.
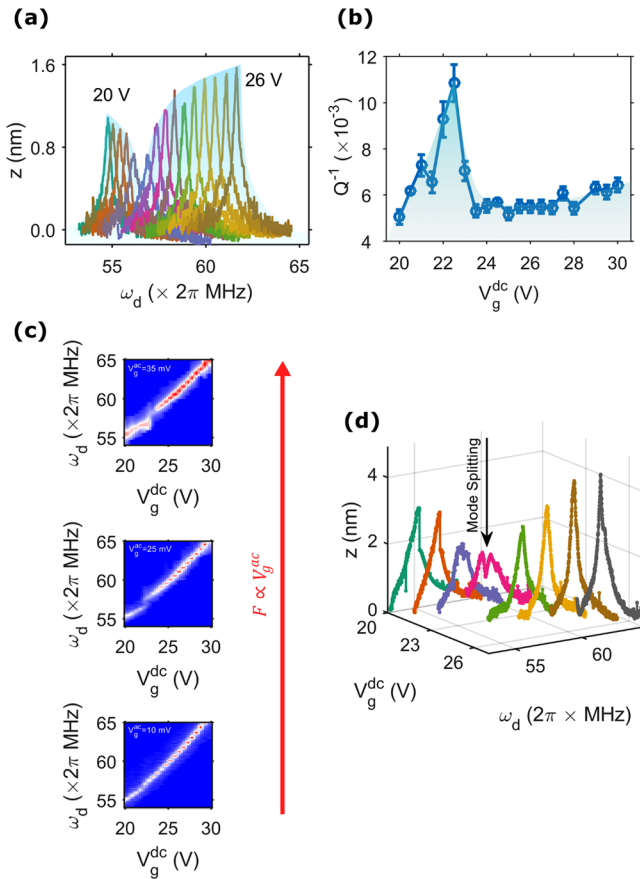
FIG. 2. (a) Amplitude response curve of mode 1 (ω_1) at multiple gate voltages. $V_g^{dc} \times V_g^{ac} = 0.2\ V^2$, which is proportional to the actuation force, is kept constant for these experiments. The shaded region shows the variation of amplitude. Amplitude is minimum at $V_g^{dc} = 22\ V$ (b) Inverse of the quality factor at different V_g^{dc}, it quantifies the damping in the system. Damping is maximum at $V_g^{dc} = 22\ V$. (c) Frequency dispersion as the actuation force is increased, peak splitting can be observed in the range $V_g^{dc} = 22\ V$ to $V_g^{dc} = 24\ V$. Peak splitting indicates mode coupling with higher order mode. (d) Amplitude vs frequency response with increasing strain (V_g^{dc}) at high actuation drive $V_g^{ac} = 35\ mV$.

To further probe this increase in damping, we perform parametric pumping by tuning the stiffness of the membrane. Parametric pumping offers an advantage in probing a mode by applying a force away from the resonant frequency and study the coupling of modes. A parametric pump can be used alone or with a direct drive. In parametric pumping, vibration amplitude is amplified by compensating the linear damping. In the simplest case, the damping can be overcome by modulating the spring constant at twice the resonance frequency.

We use the following equation of motion to describe the parametric amplification in our system:[11]

$$m\ddot{z} + \gamma \dot{z} + m\,\omega_0^2 z + \eta\,\dot{z}\,z^2 + \alpha_{eff}\,z^3 = F(\omega\,t) + F_p(2\,\omega\,t)\,z, \quad (1)$$

where m is the mass of the system γ is the linear damping, ω_0 is the resonance frequency, η is the nonlinear damping coefficient, α_{eff} is the effective Duffing nonlinearity coefficient, F is the direct force applied

at the frequency ω, the term containing F_p is the parametric force acting on the system at the frequency 2ω, and z is the vibration amplitude.

To study parametric amplification, we apply an alternating voltage (V_p^{ac}) at twice the resonance frequency of mode 1 at the gate in addition to V_g^{ac} [see Fig. 1(a)]. In a parametric system, there exists a critical pumping force beyond which the system overcomes linear damping and reaches an unstable region also known as Mathew's tongue.[11,30] The critical pump force can be measured by sweeping V_p^{ac} near 2ω. Figure 3(a) shows amplitude response using parametric drive beyond critical pump voltage (V_p^{ac0}) for different V_g^{dc}. Beyond the critical pumping, the amplitude response is governed by the nonlinear parameters and offers an excellent regime to probe the nonlinear coefficients. There are two dominant nonlinearities present in our device, namely, Duffing nonlinearity (α_{eff}) and nonlinear damping (η). The parametric response at different gate voltages indicates that α_{eff} changes from positive to negative around $V_g^{dc} \sim 24\ V$. This near cancelation of nonlinearities allows us to probe the effect of nonlinear damping by minimizing the effect of the prominent geometric nonlinearity. Figures 3(b) and 3(c) show amplitude vs frequency response far away from $V_g^{dc} \sim 24\ V$ and α_{eff} in the two cases is different. Figure 3 (d) shows the computed value of α_{eff} using the continuum model (see the supplementary material). The variation of computed α_{eff} matches well with our experimental findings. Figure 3(a) also shows a decrease in amplitude response at around $V_g^{dc} \sim 24\ V$. The variation in amplitude response is similar to the experimental findings shown in Fig. 2(a). Previously, it has been shown that the amplitudes in the parametric regime are saturated by nonlinearities present in the system.[31] To probe the nonlinear damping, we perform parametric amplification and observe the amplitude gain in the system.

In parametric amplification, the gain ($G = \frac{z_{on}}{z_{off}}$) is defined as the amplitude ratio when V_p^{ac} is ON and OFF. Figure 4(a) shows parametric gain with V_p^{ac} for different V_g^{dc}. It shows that gain increases steadily and get saturated after the critical pumping voltage. The maximum
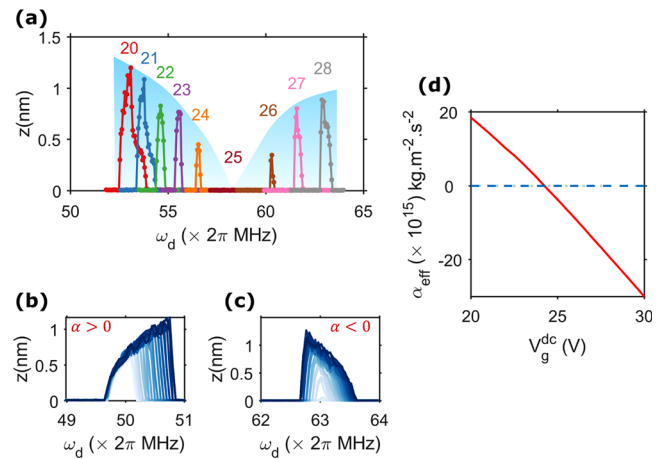

FIG. 3. Tuning of Duffing nonlinearity (α_{eff}): (a) amplitude response with frequency for different V_g^{dc} with $V_p^{ac} = 500\ mV$ and $V_g^{ac} = 0$. Change in the shape of amplitude response shows variation in nonlinearity. Amplitude response with increasing parametric force at (b) $V_g^{dc} = 16\ V$, $\alpha_{eff} > 0$ and (c) $V_g^{dc} = 28\ V$, $\alpha_{eff} < 0$. (d) The red line is α_{eff} calculated using the continuum model, it crosses the $\alpha_{eff} = 0$ (blue line) around $V_g^{dc} = 24\ V$, which matches the experimental observation in (a).
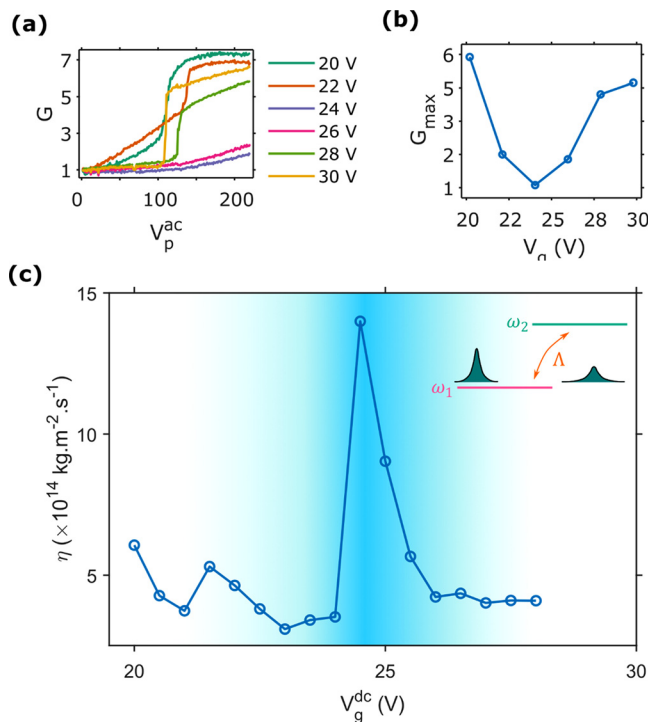
(a)

(b)

(c)

FIG. 4. Parametric amplification: (a) amplitude gain (G) vs applied pump strength V_p^{ac} for multiple V_g^{dc}. Gain increases as pump strength increases, eventually saturating due to nonlinear effects. (b) Maximum gain (G_{max}) at the start of instability tongue vs V_g^{dc}. G_{max} decreases in the region $V_g^{dc} = 22$ V to $V_g^{dc} = 26$ V. (c) Coefficient of nonlinear damping η calculated using the parametric model using Eq. (1). A higher value of η is observed in the shaded region close to $V_g^{dc} = 24$ V. Inset: schematic of the strong coupling facilitating energy dissipation channel from mode 1 to mode 2 resulting in enhanced damping. Λ represent the coupling strength. Simulation, explaining internal resonance in parametric regime, is described in the supplementary material.

gain G_{max} obtained is shown in Fig. 4(b). It shows that the G_{max} decreases significantly in the region $V_g^{dc} = 22$ to $V_g^{dc} = 26$ V. The G_{max} at $V_g^{dc} = 24$ V is ∼6 lower than G_{max} at $V_g^{dc} = 20$ V.

To understand the low gain around $V_g^{dc} = 24$ V, we calculate the nonlinear damping coefficients using the following relation: $\eta \propto \frac{2(F_pQ-2)}{z_{max}^2}$, where F_p is the parametric force, Q is the quality factor, and z_{max} is the maximum amplitude.[11] The relation allows us to estimate the coefficient of nonlinear damping from amplitude response in the parametric regime. Figure 4(c) shows the coefficient of the nonlinear damping extracted for different gate voltages.

We observe that the nonlinear damping increases significantly around $V_g^{dc} = 24$ V in parametric regime. A similar enhancement in the damping is also observed in the case of direct driving [see Figs. 2(a) and 2(b)]. Enhancement of nonlinear damping is evident, as suggested by a decrease in amplitude during direct drive and the gain during parametric amplification. We observe that the enhancement of the coefficient of nonlinear damping occurs in the region of strong internal resonance condition. In internal resonance, the two modes are coupled, providing pathways for energy exchange. In the vicinity of IR, mode 1 dissipates energy to mode 2 enhancing the nonlinear damping. Enhanced damping using dispersive coupling has been previously

reported in an engineered micro resonator coupled to a nanoresonator.[5] We find that the tunability of nonlinear damping in our experiment is similar to results reported in graphene drum resonators where 2:1 internal resonance has been observed.[9] In our experiment, a 2D nanodrum resonator accommodates modes with integer frequency ratio. The modes are coupled via tension, which facilitates tunable nonlinear damping in a single nanoresonator.

In summary, we study complex nonlinear phenomenon in a MoS$_2$ drum resonator using direct and parametric actuation drive. We identify two prominent tunable modes in the 50–200 MHz range that are coupled to each other through tension in the membrane. Dominant nonlinear coefficients α_{eff} and η are tunable in our device using a DC gate voltage. We tune the modes such that it facilitates internal resonance and energy exchange. We observe that the nonlinear damping increases significantly in the vicinity of internal resonance, η reaching as high as 15×10^{14} kg m^{-2}s^{-1} in MoS$_2$ drum resonator. In our experiment, minimizing the effect of α_{eff} helps us to probe the nonlinear damping efficiently. A highly tunable nanoresonator device such as the one presented here offers improved control of the nonlinear coefficients and enables detailed study of their dynamics. Our experiment sheds light on the possible underlying physics of nonlinear damping in oscillating systems. The parametric regime provides an excellent approach to probing the nonlinear effects by tuning the fundamental parameters such as stiffness. Tunable damping via η would be useful where dynamical damping is desired. Complex nonlinear phenomena such as fractals, and chaos could be studied using the present 2D tunable devices.[32,33]

See the supplementary material for calculations related to effective Duffing nonlinearity and nonlinear damping.

AUTHOR DECLARATIONS
Conflict of Interest

The authors have no conflicts to disclose.

Author Contributions

Parmeshwar Prasad: Conceptualization (equal); Data curation (equal); Formal analysis (equal); Investigation (equal); Methodology (equal); Software (equal); Visualization (equal); Writing – original draft (equal); Writing – review & editing (equal). **Nishta Arora:** Data curation (supporting); Formal analysis (supporting); Investigation (supporting); Methodology (equal); Validation (supporting); Writing –

08 February 2024 09:19:31

DATA AVAILABILITY

The data that support the findings of this study are available from the corresponding authors upon reasonable request.

REFERENCES

[1]C. Seoánez, F. Guinea, and A. H. Castro Neto, "Surface dissipation in nanoelectromechanical systems: Unified description with the standard tunneling model and effects of metallic electrodes," Phys. Rev. B **77**(12), 125107 (2008).

[2]R. Lifshitz and M. L. Roukes, "Thermoelastic damping in micro- and nanomechanical systems," Phys. Rev. B **61**(8), 5600–5609 (2000).

[3]P. Mohanty, D. A. Harrington, K. L. Ekinci, Y. T. Yang, M. J. Murphy, and M. L. Roukes, "Intrinsic dissipation in high-frequency micromechanical resonators," Phys. Rev. B **66**(8), 085416 (2002).

[4]I. Wilson-Rae, "Intrinsic dissipation in nanomechanical resonators due to phonon tunneling," Phys. Rev. B **77**(24), 245418 (2008).

[5]I. Mahboob, N. Perrissin, K. Nishiguchi, D. Hatanaka, Y. Okazaki, A. Fujiwara, and H. Yamaguchi, "Dispersive and dissipative coupling in a micromechanical resonator embedded with a nanomechanical resonator," Nano Lett. **15**(4), 2312–2317 (2015).

[6]A. Eichler, J. Moser, J. Chaste, M. Zdrojek, I. Wilson-Rae, and A. Bachtold, "Nonlinear damping in mechanical resonators based on graphene and carbon nanotubes," Nat. Nanotechnol. **6**(6), 339–342 (2011).

[7]J. Güttinger, A. Noury, P. Weber, A. M. Eriksson, C. Lagoin, J. Moser, C. Eichler, A. Wallraff, A. Isacsson, and A. Bachtold, "Energy-dependent path of dissipation in nanomechanical resonators," Nat. Nanotechnol. **12**(7), 631–636 (2017).

[8]A. Eichler, J. Chaste, J. Moser, and A. Bachtold, "Parametric amplification and self-oscillation in a nanotube mechanical resonator," Nano Lett. **11**(7), 2699–2703 (2011).

[9]A. Keşkekler, O. Shoshani, M. Lee, H. S. J. van der Zant, P. G. Steeneken, and F. Alijani, "Tuning nonlinear damping in graphene nanoresonators by parametric–direct internal resonance," Nat. Commun. **12**(1), 1099 (2021).

[10]J. Atalaya, T. W. Kenny, M. L. Roukes, and M. I. Dykman, "Nonlinear damping and dephasing in nanomechanical systems," Phys. Rev. B **94**(19), 195440 (2016).

[11]R. Lifshitz and M. C. Cross, *Reviews of Nonlinear Dynamics and Complexity* (Wiley-VCH Verlag GmbH & Co. KGaA, Weinheim, Germany, 2008).

[12]C. Samanta, N. Arora, and A. K. Naik, "Tuning of geometric nonlinearity in ultrathin nanoelectromechanical systems," Appl. Phys. Lett. **113**(11), 113101 (2018).

[13]M. Amabili, P. Balasubramanian, I. Bozzo, I. D. Breslavsky, G. Ferrari, G. Franchini, F. Giovanniello, and C. Pogue, "Nonlinear dynamics of human aortas for material characterization," Phys. Rev. X **10**(1), 011015 (2020).

[14]B. Divinskiy, S. Urazhdin, S. O. Demokritov, and V. E. Demidov, "Controlled nonlinear magnetic damping in spin-Hall nano-devices," Nat. Commun. **10**(1), 5211 (2019).

[15]L. Mandel and E. Wolf, *Optical Coherence and Quantum Optics* (Cambridge University Press, 1995).

[16]Z. R. Lin, Y. Nakamura, and M. I. Dykman, "Critical fluctuations and the rates of interstate switching near the excitation threshold of a quantum parametric oscillator," Phys. Rev. E **92**(2), 022105 (2015).

[17]Z. Leghtas, S. Touzard, I. M. Pop, A. Kou, B. Vlastakis, A. Petrenko, K. M. Sliwa, A. Narla, S. Shankar, M. J. Hatridge, M. Reagor, L. Frunzio, R. J. Schoelkopf, M. Mirrahimi, and M. H. Devoret, "Confining the state of light to a quantum manifold by engineered two-photon loss," Science **347**(6224), 853–857 (2015).

[18]S. Zaitsev, O. Shtempluck, E. Buks, and O. Gottlieb, "Nonlinear damping in a micromechanical oscillator," Nonlinear Dyn. **67**(1), 859–883 (2012).

[19]V. Singh, O. Shevchuk, Y. M. Blanter, and G. A. Steele, "Negative nonlinear damping of a multilayer graphene mechanical resonator," Phys. Rev. B **93**(24), 245407 (2016).

[20]M. Imboden, O. Williams, and P. Mohanty, "Nonlinear dissipation in diamond nanoelectromechanical resonators," Appl. Phys. Lett. **102**(10), 103502 (2013).

[21]S. Schmid, L. G. Villanueva, and M. L. Roukes, *Fundamentals of Nanomechanical Resonators* (Springer International Publishing, Cham, 2016).

[22]H. Farokhi, R. T. Rocha, A. Z. Hajjaj, and M. I. Younis, "Nonlinear damping in micromachined bridge resonators," Nonlinear Dyn. **111**(3), 2311–2325 (2023).

[23]X. Dong, M. I. Dykman, and H. B. Chan, "Strong negative nonlinear friction from induced two-phonon processes in vibrational systems," Nat. Commun. **9**(1), 3241 (2018).

[24]A. Croy, D. Midtvedt, A. Isacsson, and J. M. Kinaret, "Nonlinear damping in graphene resonators," Phys. Rev. B **86**(23), 235435 (2012).

[25]P. Prasad, N. Arora, and A. K. Naik, "Gate tunable cooperativity between vibrational modes," Nano Lett. **19**(9), 5862–5867 (2019).

[26]J. P. Mathew, R. N. Patel, A. Borah, R. Vijay, and M. M. Deshmukh, "Dynamical strong coupling and parametric amplification in mechanical modes of graphene drums," Nat. Nanotechnol. **11**(9), 747–751 (2016).

[27]H. C. Nathanson and R. A. Wickstrom, "A resonant-gate silicon surface transistor with high-q band-pass properties," Appl. Phys. Lett. **7**(4), 84–86 (1965).

[28]D. W. Carr and H. G. Craighead, "Fabrication of nanoelectromechanical systems in single crystal silicon using silicon on insulator substrates and electron beam lithography," J. Vac. Sci. Technol., B **15**(6), 2760–2763 (1997).

[29]N. Arora and A. K. Naik, "Qualitative effect of internal resonance on the dynamics of two-dimensional resonator," J. Phys. D: Appl. Phys. **55**(26), 265301 (2022).

[30]A. H. Nayfeh and D. T. Mook, *Nonlinear Oscillations* (Wiley-VCH Verlag GmbH, Weinheim, Germany, 1995).

[31]R. Lifshitz and M. C. Cross, "Response of parametrically driven nonlinear coupled oscillators with application to micromechanical and nanomechanical resonator arrays," Phys. Rev. B **67**(13), 134302 (2003).

[32]Y.-H. Kao and C.-S. Wang, "Analog study of bifurcation structures in a Van Der Pol oscillator with a nonlinear restoring force," Phys. Rev. E **48**(4), 2514 (1993).

[33]A. Venkatesan and M. Lakshmanan, "Nonlinear dynamics of damped and driven velocity-dependent systems," Phys. Rev. E **55**(5), 5134 (1997).

08 February 2024 09:19:31